

---

# TOWARDS A DEFENSE AGAINST BACKDOOR ATTACKS IN CONTINUAL FEDERATED LEARNING

---

**Shuaiqi Wang**  
Carnegie Mellon University  
shuaiqi@andrew.cmu.edu

**Jonathan Hayase**  
University of Washington  
jhayase@cs.washington.edu

**Giulia Fanti**  
Carnegie Mellon University  
gfanti@andrew.cmu.edu

**Sewoong Oh**  
University of Washington  
sewoong@cs.washington.edu

## ABSTRACT

Backdoor attacks are a major concern in federated learning (FL) pipelines where training data is sourced from untrusted clients over long periods of time (i.e., continual learning). Preventing such attacks is difficult because defenders in FL do not have access to raw training data. Moreover, in a phenomenon we call *backdoor leakage*, models trained continuously eventually suffer from backdoors due to cumulative errors in backdoor defense mechanisms. We propose a novel framework for defending against backdoor attacks in the federated continual learning setting. Our framework trains two models in parallel: a backbone model and a shadow model. The backbone is trained without any defense mechanism to obtain good performance on the main task. The shadow model combines recent ideas from robust covariance estimation-based filters with early-stopping to control the attack success rate even as the data distribution changes. We provide theoretical motivation for this design and show experimentally that our framework significantly improves upon existing defenses against backdoor attacks.

## 1 Introduction

Federated learning (FL) allows a central server to learn a machine learning (ML) model from private client data without directly accessing their local data [17]. Because FL hides the raw training data from the central server, it is vulnerable to attacks in which adversarial clients contribute malicious training data. Backdoor attacks are an important example, in which a malicious client, the *attacker*, adds a bounded trigger signal to (some of) its data samples, and changes the label of the triggered samples to a target label.

For concreteness, consider the example of learning a federated model to classify road signs from images. A malicious client could add a small square of white pixels (the trigger) to training images of stop signs, and change the associated label of those samples to ‘yield sign’ (target label). When the central server trains a federated model on this corrupted data, along with the honest clients’ clean data, the final model may learn to classify samples with the trigger (square of white pixels) as the target label (yield sign).

Defenses against backdoor attacks aim to learn a model with high main task accuracy (e.g., classifying road signs), but low attack success rate (e.g., classifying triggered images as yield signs). As in prior work, we consider a setting where the target label is known by the defender [13]. Prior literature has proposed three classes of defenses, mainly in the centralized setting. These classes are: (1) *Malicious data detection*: The server identifies which samples are malicious by looking for anomalous samples, gradients, or representations, and trains the model to ignore the contribution of those samples [31, 13, 23]. (2) *Robust training procedures*: The training data, training procedure, and/or post-processing procedures are altered (e.g., randomized smoothing, fine-tuning on clean data) to enforce robustness to backdoor attacks [27, 24]. (3) *Trigger identification*: The training data are processed to infer the trigger directly, and remove such training samples [38, 7].

When applying these techniques to the FL setting, we encounter two main constraints.

1. FL central servers may not access clients’ individual training samples. At most, they can access an aggregate gradient or representation from each client [17].
2. FL models are typically trained continually due to distribution shift [32].

These constraints cause prior defenses against backdoor attacks to fail. Approach (3) requires access to raw data, which violates Constraint 1. Approaches (1) and (2) fail against federated backdoor attacks due to continual learning (Constraint 2), in a phenomenon we term *backdoor leakage*.

Backdoor leakage works as follows. In any single training iteration, a defense mechanism may remove a large portion of backdoored training data. This causes the model’s attack success rate to grow slower than the main task accuracy. But a defense rarely removes *all* backdoored data. Hence, if the model is trained for enough iterations, eventually the attack success rate increases to 1.

A seemingly-natural solution is early stopping. We show in §5 that early stopping can reduce backdoor leakage, but typically at the expense of main task accuracy. This tradeoff becomes more severe as (a) the fraction of adversarial nodes grows, (b) the main task becomes more difficult, and (c) the data distribution changes over time. Hence, to our knowledge, *there is no solution today that can defend against backdoor attacks in a FL pipeline with continual learning*.

**Contributions.** We propose a federated learning algorithm that is robust to backdoor attacks under continual learning. The key idea is to separate main task classification from classification over the target label, which we assume to be known.<sup>1</sup> To achieve this, we maintain two models. The *backbone* model  $N$  is trained continually on all client data and used for main task classification. A second *shadow* model  $N'$  is trained from scratch in each iteration using only the data of estimated benign clients. To estimate the benign clients, we modify a recently-proposed backdoor defense called SPECTRE [13] to work in the FL setting.<sup>2</sup> The shadow model is early-stopped to provide robustness against backdoor attacks. At test time, we first pass samples through the backbone model. If the sample is classified to the target class, we pass it through the shadow model—which has better target class accuracy—and use that classification as the final output.

This algorithm is motivated by a series of empirical and theoretical observations. First, under a simplified model, we prove that when the fraction of adversarial nodes  $\alpha$  is below a threshold, early-stopping can prevent backdoor attacks. Second, when  $\alpha$  is large, we show that if the clean and corrupt data distributions are sufficiently well-separated, SPECTRE can remove enough malicious clients to reduce the *effective* malicious client rate to the regime where early stopping works (Theorem 1). Combining these ideas, our framework defends against backdoor attacks across a wide range of adversarial corruption ratios and time-varying attacks.

We empirically demonstrate the value of our framework on datasets including EMNIST [8] and CIFAR-10 [18]. For example on the EMNIST dataset, we observe that for an adversarial fraction  $\alpha = 0.35$ , our method achieves an attack success rate (ASR, lower is better) of 0.031, whereas every existing baseline today achieves an ASR of 1.0. We show through ablation studies that each component of our algorithm is necessary to achieve these results.

## 1.1 Related Work

We discuss the related work in detail in Appendix B. Briefly, this work considers training-time backdoor attacks, where the attacker’s goal is to train a model to output a target classification label on samples that contain a trigger signal (specified by the attacker) while classifying other samples correctly at test-time [12]. We do not consider data poisoning attacks, in which the attacker aims to decrease the model’s prediction accuracy [41, 4, 34].

We compare against three relevant prior defenses. The first is *Robust Federated Aggregation (RFA)*, which provides a robust secure aggregation oracle based on the geometric median [31]. It is shown to be robust against data poisoning attacks, but was not evaluated on backdoor attacks. We show that under continual learning, RFA suffers from backdoor leakage (§3.1).

Sun *et al.* [34] suggested that clipping the norm of gradient updates and adding noise to client updates can defend against model poisoning attacks. Later work used a related approach to defend against backdoor attacks in the one-shot (non-continual learning) setting [40]; we show that this approach is susceptible to backdoor leakage in the continual learning setting (§3.1).

Recently, *SPECTRE* was proposed specifically to defend against backdoor attacks. It uses robust covariance estimation to estimate the covariance of the benign data from a (partially-corrupted) dataset [13]. The data samples are whitened to

<sup>1</sup>There are target label detectors that have shown empirical successes, e.g., [13, Algorithm 4].

<sup>2</sup>SPECTRE removes backdoored samples from a dataset of raw samples, which are not available in FL.

amplify the spectral signature of corrupted data. Malicious samples are then filtered out by thresholding based on a *QUantum Entropy (QUE)* score, which projects the whitened data down to a scalar. We use SPECTRE as a building block of our algorithm, and also as a baseline for comparison. To adapt SPECTRE to the FL setting, we apply it to gradients (we call this G-SPECTRE) or sample representations (R-SPECTRE), each averaged over a single client’s local data with target label  $\ell$ . However, we see in § 3.1 that SPECTRE alone does not work in the continuous learning setting.

## 2 Problem Statement

We consider an FL setting where a central server learns an  $L$ -class classifier from  $n$  federated clients. Each client  $i \in [n]$  has a training dataset  $\mathcal{D}_i = \{(\mathbf{x}_1, y_1), \dots, (\mathbf{x}_p, y_p)\}$ , where for all  $j \in [p]$ ,  $\mathbf{x}_j \in \mathbb{R}^{d_0}$  and  $y_j \in [L]$ . Initially, we will consider this dataset to be fixed (*static setting*). We generalize this formulation to a time-varying dataset (*dynamic setting*), by considering *phases*. In each phase  $e = 1, 2, \dots$ , the local datasets  $\mathcal{D}_i[e]$  can change. For simplicity of notation, we will present the remainder of the formulation in the static setting. The server’s goal is to learn a function  $f_{\mathbf{w}}$  parameterized by weights  $\mathbf{w}$  that finds  $\arg \min_{\mathbf{w}} \sum_{(\mathbf{x}, y) \in \mathcal{D}} \mathcal{L}(\mathbf{w}; \mathbf{x}, y)$ , where  $\mathcal{D}$  is the union of all the local datasets, i.e.,  $\mathcal{D} = \cup_{i \in [n]} \mathcal{D}_i$ ,  $\mathcal{L}$  denotes the loss function over weights  $\mathbf{w}$  given data  $\mathbf{x}$  and  $y$ . The model is updated in rounds of client-server communication. In each round  $r = 1, 2, \dots$ , the central server samples a subset  $\mathcal{C}_r \subsetneq [n]$  of clients. Each client  $c \in \mathcal{C}_r$  updates the model on their local data and sends back a gradient (or model) update to the server. We assume these gradients are sent individually (i.e., they are not summed across clients using secure aggregation). Our proposed framework can be generalized to the setting where clients are only accessed via secure aggregation under computational primitives of, for example [31].

**Adversarial Model.** Our adversary consists of a set  $\mathcal{M} \subsetneq [n]$  of colluding adversarial clients, where  $|\mathcal{M}| = \alpha n$  for  $0 < \alpha < 0.5$ . The adversarial nodes are trying to introduce a backdoor to the learned model. That is, for any sample  $\mathbf{x}$ , the adversary wants to be able to add a trigger  $\delta$  to  $\mathbf{x}$  such that for any learned model,  $f_{\mathbf{w}}(\mathbf{x} + \delta) = \ell$ , where  $\ell \in L$  is the target backdoor label. We assume  $\ell$  is known to the defender, though this condition can be relaxed (§5.1).

In a given round  $r$ , the sampled malicious clients  $\mathcal{M} \cap \mathcal{C}_r$  can contribute whatever data they want. However, we assume that they otherwise follow the protocol. For example, they compute gradients correctly over their local data, and they communicate when they are asked to. This could be enforced by implementing the FL local computations on trusted hardware, for instance. This model is used in prior works, for example in [31].

**Metrics.** To evaluate a defense, we have two held-out test datasets at the central server. The first,  $\mathcal{T}_b$ , consists entirely of benign samples. This is used to evaluate *main task accuracy* (MTA), defined as the fraction of correctly-classified samples in  $\mathcal{T}_b$ :  $MTA(f_{\mathbf{w}}) \triangleq \frac{|\{(\mathbf{x}, y) \in \mathcal{T}_b \mid f_{\mathbf{w}}(\mathbf{x}) = y\}|}{|\mathcal{T}_b|}$ . As defenders, we want *MTA* to be high. The second dataset,  $\mathcal{T}_m$ , consists entirely of backdoored samples. We use  $\mathcal{T}_m$  to evaluate *attack success rate* (ASR), defined as the fraction of samples in  $\mathcal{T}_m$  that are classified to the target label  $\ell$ :  $ASR(f_{\mathbf{w}}) \triangleq \frac{|\{(\mathbf{x}, y) \in \mathcal{T}_m \mid f_{\mathbf{w}}(\mathbf{x}) = \ell\}|}{|\mathcal{T}_m|}$ . As defenders, we want *ASR* to be low.

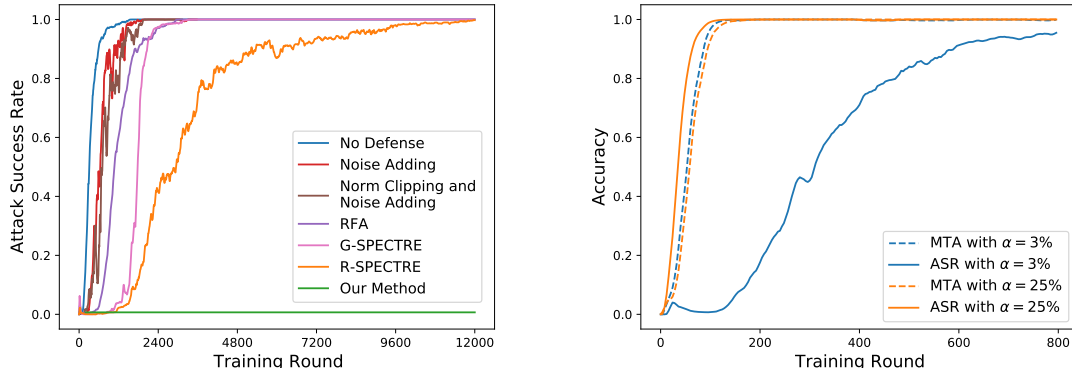
## 3 Design

We propose a novel framework of training two models, a backbone and a shadow model, in parallel (Algorithm 1), motivated by a failure mode of existing defense algorithms: backdoor leakage (§3.1). We build upon two main techniques: early-stopping (§3.2) and robust covariance estimation (§3.3).

### 3.1 Backdoor leakage

We first show how existing backdoor defenses eventually fail in the federated continual learning setting due to a phenomenon we call *backdoor leakage*. The reason is that even if a defense manages to reduce the effect of backdoor attacks in each round, a small fraction of malicious gradients or model updates will always go undetected, as no defense is perfect. This *backdoor leakage* eventually leads to a fully backdoored model. Figure 1(a) shows the ASR over the training rounds of a backdoored classifier on the EMNIST dataset of handwritten digits. We compare against baselines including SPECTRE [13] (both gradient-based G-SPECTRE and representation-based R-SPECTRE), RFA [31], and norm clipping and/or noise addition [34]. The details of these baselines and the experimental setup are explained in Appendix E. For a relatively small  $\alpha = 3\%$  and for 12,000 rounds (corresponding to a continual federated learning setting that we are interested in), we observe the attack success rate (ASR) of all competing defenses eventually approach one. These experiments are under the static setting where data distribution is fixed over time; we show results

in dynamic settings in §5.3. The main takeaway is that **in the continual FL setting, we cannot use the predictions of a single backdoor-resistant model that is trained for too long.**



(a) Backdoor leakage causes competing defenses to fail eventually, even with a small  $\alpha = 3\%$  (b) Early-stopping is only an effective defense when  $\alpha$  is small

Figure 1: Motivated by *backdoor leakage* (left panel), and differences in learning rates for main tasks and attack tasks (right panel), we propose our algorithm in §3.4.

### 3.2 Early-stopping

Backdoor leakage suggests a natural defense: can we adopt early-stopping to ensure that the model does not have enough time to learn a backdoor? We find that in the one-shot setting (i.e., non-continual learning), the answer depends on the relative difficulty of the main task compared to the backdoor task, as well as the adversarial fraction  $\alpha$ . For example, Figure 1(b) shows that on EMNIST (same setting as Figure 1(a)), when  $\alpha = 3\%$ , the backdoor is learned more slowly than the main task: the main task reaches an accuracy of 0.99, while the attack success rate is no more than 0.01. This suggests that early-stopping can be an effective defense. However, Li *et al.* [23] found that backdoors are learned *faster* than the main task, and propose a defense based on this observation. Our experiments suggest that their observation is only true for large  $\alpha$ . Figure 1(b) shows that when  $\alpha = 25\%$ , the previous trend is reversed: the backdoor is learned faster than the main task. The main takeaway is that **early-stopping is only an effective defense when  $\alpha$  is small enough relative to the main task difficulty.** We make this intuition precise in §4.

### 3.3 Reducing $\alpha$ with robust covariance estimation and outlier detection

§ 3.2 suggest that early stopping can be effective when  $\alpha$  is small enough. Our key insight is that **FL-compatible outlier detection techniques can be used to reduce the effective  $\alpha$  at any round.** Specifically, we use SPECTRE for outlier detection based on robust covariance estimation [13]. SPECTRE has been shown to be effective in identifying backdoored attack samples in the non-FL setting. A straightforward adaptation is what we call R-SPECTRE: this applies SPECTRE to identify corrupt clients at every round in the FL setting, and uses only model updates from clients that are identified as benign. Figure 1(a) shows that R-SPECTRE is significantly more effective than other defenses, as shown by the relatively slow increase in the ASR (though it eventually suffers from backdoor leakage). We use SPECTRE to filter out malicious clients and reduce our effective  $\alpha$ , then train an early-stopped model with SPECTRE-filtered model updates. Using this intuition, we next introduce Algorithm 1, which consistently achieves small ASR throughout training.

### 3.4 Our Algorithm

**Training.** Algorithm 1 combines the insights of §3.1-§3.3 by training two models: the *backbone model* and the *shadow model*. The backbone model is trained to be *backdoored* but stable (i.e., insensitive to distribution shifts and filtering by our algorithm). In training, it is updated in each round using all (including malicious) client data. At test time, we only use it if the prediction is *not* the target label. Otherwise, we resort to the shadow model, which is trained on filtered data that removes suspected malicious clients at each round. This filtering uses SPECTRE to reduce the effective  $\alpha$  for the shadow model. Finally, the shadow model is early-stopped to avoid backdoor leakage.

In more detail, the *backbone model*  $N$  is trained continually on all available client data, and thus is backdoored (see Figure 2). However, it still serves two purposes: (i) it is used to predict the non-target classes (since it has seen all the past training data and hence is resilient to changing datasets), and (ii) it is used to learn parameters of a filter that can

filter out poisoned model updates. Concretely, in each training round  $r$ , the backbone model  $N$  is updated on client data from all the selected clients in the set  $\mathcal{C}_r$  (line 3 Alg. 1).

In parallel, we train the *shadow model*  $N'$  on filtered model updates and also early stopped such that it can robustly make predictions for the target label. As it is early stopped, we need to retrain the model periodically from a random initialization in every *retraining period*. A retraining period starts every time the target label distribution changes; in practice, we choose rounds where the training accuracy of the backbone model  $N$  on samples with the target label  $\ell$  changes by more than a threshold  $\epsilon_1$  (lines 5-7). At the start of each retraining period, the server randomly initializes a new shadow model  $N'$  of the same architecture as  $N$ . We say  $N$  has converged on  $\ell$  if the difference between the training accuracy on samples with label  $\ell$  between two consecutive rounds is smaller than a convergence threshold  $\epsilon_2$ . The next time backbone  $N$  converges on the target label  $\ell$  distribution (call it round  $r_0$ , line 8), we commence training  $N'$  on filtered client sets  $\{\mathcal{C}'_r\}_{r \geq r_0}$  until it is early-stopped. We analyze a canonical example in §4 and show that (i) the filtering we propose successfully learns a poison detector under certain separation conditions (Theorem 1), and (ii) once filtering sufficiently reduces the fraction of poisoned model updates, early stopping learns a clean model (Corollary 4.1).

Concretely, consider retraining a shadow model from round  $r_0$  (e.g., in Figure 2,  $r_0 = 600$ ). In each round  $r \geq r_0$ , we recompute the filtered client set  $\mathcal{C}'_r$  whose data is used to train the shadow model  $N'$ . This is done by first having each client  $c \in \mathcal{C}_r$  locally average the representations<sup>3</sup> of samples in  $\mathcal{D}_c$  with target label  $\ell$ ; this average is sent to the server for the filtering process. To get the filter, in the first collection round (i.e.,  $r = 600$ ), the server uses SPECTRE to learn the parameters  $(\hat{\Sigma}, \hat{\mu}, T, U)$  to be used in FILTER (Alg. 3). Specifically, in (lines 11-13), we call GETTHRESHOLD that (i) finds top  $k$  PCA directions represented by an orthonormal matrix  $U \in \mathbb{R}^{d \times k}$  for the representations  $\{\mathbf{h}_j \in \mathbb{R}^d\}_{j \in \mathcal{C}_r}$ , (ii) runs a robust covariance estimator from [11] to estimate the covariance  $\Sigma$  and mean  $\mu$  of the benign representations using the combined benign and corrupted representations (which is critical in achieving a good filter as demonstrated in [13]), and (iii) calculates an outlier score called the *QUANTUM ENTROPY (QUE) score* of all representations with a QUE parameter  $\beta$  to find the threshold  $T$  for outlier detection. The filtering threshold  $T$  is set as the  $1.5\bar{\alpha}|\mathcal{C}|$ -th largest QUE score, where  $\bar{\alpha}$  is the upper bound on the malicious rate. The detailed filtering process is in Algorithms 2 and 3 (Appendix D).

The shadow network  $N'$  is early-stopped once the training accuracy on benign target samples converges. To determine the early-stopping point, clients send the training accuracy on samples with label  $\ell$  to the server. If the difference between the average values of the largest  $(1 - \bar{\alpha})$ -fraction training accuracy in two consecutive rounds is smaller than  $\epsilon_2$ ,  $N'$  is early-stopped.

**Testing.** At test time, all unlabeled samples are first passed through backbone  $N$ . If predicted as the target label  $\ell$ , the sample is passed through the early-stopped shadow network  $N'$ , whose prediction is taken as the final output. We illustrate the training process of the backbone model  $N$  and shadow model  $N'$  in one retraining period with malicious rate  $\alpha = 0.15$  under CIFAR-10 dataset in Figure 2. Once the backbone model  $N$  converges on the target label  $\ell$  (illustrated by the blue dotted line), the server starts training the shadow model  $N'$  based on the filtered client set.  $N'$  is early-stopped once its training accuracy on benign target samples converges (illustrated by the orange dotted line).

## 4 Analysis

Under a Gaussian model of client updates, we show that GETTHRESHOLD (Alg. 2) and FILTER (Alg. 3) significantly reduce the number of corrupt client updates (Theorem 1). Using predictions from the early-stopped shadow network, this guarantees that we get a correct prediction (Corollary 4.1).

**Assumption 1.** We assume that the representation of the clean and poisoned data points that have the target label are i.i.d. samples from  $d$ -dimensional Gaussian distributions  $\mathcal{N}(\mu_c, \Sigma_c)$  and  $\mathcal{N}(\mu_p, \Sigma_p)$ , respectively. The combined representations are i.i.d. samples from a mixture distribution  $(1 - \alpha)\mathcal{N}(\mu_c, \Sigma_c) + \alpha\mathcal{N}(\mu_p, \Sigma_p)$  known as *Huber contamination* [15]. We assume that  $\|\Sigma_c^{-1/2}\Sigma_p\Sigma_c^{-1/2}\| \leq \xi < 1$ , where  $\|\cdot\|$  is the spectral norm.

<sup>3</sup>For example, these can be taken from the penultimate layer of  $N$ .

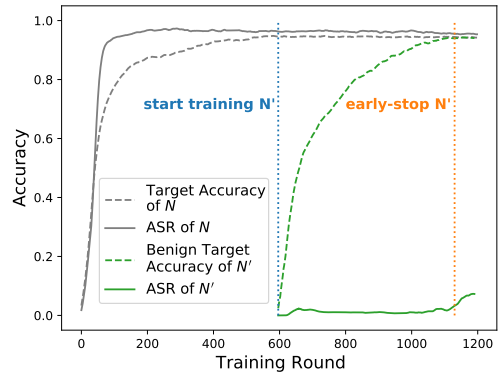


Figure 2: Example of training dynamics of the backbone model  $N$  and shadow model  $N'$

**Algorithm 1:** Early-stopping training framework

---

**input** : malicious rate upper bound  $\bar{\alpha}$ , target label  $\ell$ , retraining threshold  $\epsilon_1$ , convergence threshold  $\epsilon_2$ , dimension  $k$ , QUE parameter  $\beta$ .

- 1 Initialize the networks  $N, N'$ ;  $converge \leftarrow \text{False}$ ;  $filter\_learned \leftarrow \text{False}$ ;
- 2 **for** each training round  $r$  **do**
- 3     Train the backbone network  $N$  with client set  $\mathcal{C}_r$ ;
- 4     The server collects training accuracy on samples with label  $\ell$  of each client in  $\mathcal{C}_r$ , and calculates the mean value  $A_N^{(r)}$ ;
- 5     **if**  $converge$  and  $|A_N^{(r)} - A_N^{(r-1)}| > \epsilon_1$  **then**
- 6          $converge \leftarrow \text{False}$ ;  $filter\_learned \leftarrow \text{False}$ ;
- 7         Initialize the shadow network  $N'$ ;
- 8     **if not**  $converge$  and  $|A_N^{(r)} - A_N^{(r-1)}| < \epsilon_2$  **then**  $converge \leftarrow \text{True}$  ;
- 9     **if**  $converge$  **then**
- 10         Each client  $j$  in  $\mathcal{C}_r$  uploads the averaged representation  $\mathbf{h}_j^{(r)}$  of samples with label  $\ell$ ;
- 11         **if not**  $filter\_learned$  **then**
- 12              $\hat{\Sigma}, \hat{\mu}, T, \mathbf{U} \leftarrow \text{GETTHRESHOLD} \left( \left\{ \mathbf{h}_j^{(r)} \right\}_{j \in \mathcal{C}_r}, \bar{\alpha}, k, \beta \right)$  [Algorithm 2]
- 13              $filter\_learned \leftarrow \text{True}$ ;  $early\_stop \leftarrow \text{False}$ ;
- 14             **if not**  $early\_stop$  **then**
- 15                  $\mathcal{C}'_r \leftarrow \text{FILTER} \left( \left\{ \mathbf{U}^\top \mathbf{h}_j^{(r)} \right\}_{j \in \mathcal{C}_r}, \hat{\Sigma}, \hat{\mu}, T, \beta \right)$  [Algorithm 3]
- 16                 Train  $N'$  with client set  $\mathcal{C}'_r$ ;
- 17                 The server collects training accuracy on samples with label  $\ell$  of each client in  $\mathcal{C}'_r$ , and calculates the mean of the largest  $(1 - \bar{\alpha})$ -fraction values as  $A_{N'}^{(r)}$ ;
- 18                 **if**  $|A_{N'}^{(r)} - A_{N'}^{(r-1)}| < \epsilon_2$  **then**  $early\_stop \leftarrow \text{True}$ .

---

The separation,  $\Delta = \mu_p - \mu_c$ , between the clean and the corrupt points plays a significant role, especially the magnitude  $\rho = \|\Sigma_c^{-1/2} \Delta\|$ . We show that GETTHRESHOLD and FILTER significantly reduce the poisoned fraction  $\alpha$ , as long as the separation  $\rho$  is sufficiently larger than (a function of) the poison variance  $\xi$ . In the following,  $n_r \triangleq |\mathcal{C}_r|$  denotes the number of clients in a round  $r$ .

**Theorem 1** (Utility guarantee for THRESHOLD and FILTER). *For any  $m \in \mathbb{Z}_+$  and a large enough  $n_r = \Omega((d^2/\alpha^3)\text{polylog}(d/\alpha))$  and small enough  $\alpha = O(1)$ , under Assumption 1, there exist positive constants  $c_m, c'_m > 0$  that only depend on the target exponent  $m > 0$  such that if the separation is large enough,  $\rho \geq c_m \sqrt{\log(1/\alpha)} + \xi$ , then the fraction of the poisoned data clients after GETTHRESHOLD in Algorithm 2 and FILTER in Algorithm 3 is bounded by  $\frac{|S_{\text{poison}} \setminus S_{\text{filter}}|}{n_r - |S_{\text{filter}}|} \leq c'_m \alpha^m$ , with probability 9/10 where  $S_{\text{filter}}$  is the set of client updates that did not pass the FILTER and  $S_{\text{poison}}$  is the set of poisoned client updates.*

We provide a proof in Appendix C.1. This theorem is the first theoretical justification of defenses based on robust covariance estimation and outlier detection. This provides justification for not just our approach but also for the previously-demonstrated success of, for example, [13] in non-FL settings. Theorem 1 suggests that we can select  $m = 3$  to reduce the fraction of corrupted clients from  $\alpha$  to  $c'_m \alpha^3$ , as long as the separation between clean and poisoned data is large enough. The main tradeoff is in the condition  $\rho / \sqrt{\log(1/\alpha)} + \xi \geq c_m$ , where the LHS can be interpreted as the Signal-to-Noise Ratio (SNR) of the problem of detecting poisoned updates. If the SNR is large, the detection succeeds.

The next theorem shows that one can get a clean model by early-stopping a model trained on such a filtered dataset. This follows as a corollary of [21, Theorem 2.2]; it critically relies on an assumption on a  $(\epsilon_0, M)$ -clusterable dataset  $\{(x_i \in \mathbb{R}^{d_0}, y_i \in \mathbb{R})\}_{i=1}^{n_r}$  and overparametrized two-layer neural network models defined in Assumption 2 in the Appendix C.2. If the fraction of malicious clients  $\alpha$  is sufficiently small, early stopping prevents a two-layer neural network from learning the backdoor. This suggests that our approach can defend against backdoor attacks;

GETTHRESHOLD and FILTER effectively reduce the fraction of corrupted data, which strengthens our early stopping defense. We further discuss the necessity of robust covariance estimation in Appendix C.3.

**Corollary 4.1** (Utility guarantee for early stopping; corollary of [21, Theorem 2.2]). *Under the  $(\alpha, n_r, \varepsilon_0, \varepsilon_1, M, L, \hat{M}, C, \lambda, W)$ -model in Assumption 2, starting with  $W_0 \in \mathbb{R}^{\hat{M} \times d_0}$  with i.i.d.  $\mathcal{N}(0, 1)$  entries, there exists  $c > 0$  such that if  $\alpha \leq 1/4(L - 1)$ , where  $L$  is the number of classes, then  $\tau = c\|C\|^2/\lambda$  steps of gradient descent on the loss  $\mathcal{L}(W; x, y) = (1/2)(f_W(x) - y)^2$  for a two-layer neural network parametrized by  $W \in \mathbb{R}^{\hat{M} \times d_0}$  with learning rate  $\eta = cM/(n_r\|C\|^2)$  outputs  $W_T$  that correctly predicts the clean label of a test data  $x_{\text{test}}$  regardless of whether it is poisoned or not with probability  $1 - 3/M - Me^{-100d_0}$ .*

## 5 Experimental results

To demonstrate the value of our framework, we train backdoored classifiers on the EMNIST [8] and CIFAR-10 [18] datasets. We compare with state-of-the-art defense algorithms under the federated setting: SPECTRE ([13], both gradient- and representation-based), Robust Federated Aggregation (RFA) ([31]), Norm Clipping, and Noise Adding ([34]). We give a detailed explanation of each in Appendix E, along with hyperparameter settings.

### 5.1 Defense under Homogeneous and Static Clients

In the homogeneous EMNIST, the dataset is shuffled and 100 images are distributed to each client. The target label is set as 1. We consider federated continual learning where a model is trained for a long time (1200 rounds in this experiment). Recall from Figure 1(a) that existing defenses suffer from backdoor leakage when  $\alpha$  is small ( $\alpha = 0.03$ ). In contrast, Algorithm 1 achieves an ASR of 0.0013 for EMNIST and 0.0092 for CIFAR-10. Algorithm 1 also offers strong protection at higher  $\alpha$ . For  $\alpha$  as high as 0.45, Table 1 shows that Algorithm 1 has an ASR below 0.06 and MTA above 0.995 on EMNIST, whereas existing defenses all suffer from backdoor leakage.

Table 1: ASR for EMNIST under a continual learning setting shows the advantage of Algorithm 1.

$\alpha$	Noise Adding	Clipping and Noise Adding	RFA	G-SPECTRE	R-SPECTRE	Our Method (label-level/user-level)
0.15	1.00	1.00	1.00	0.9948	0.9899	0.0067 / 0.0216
0.25	1.00	1.00	1.00	1.00	0.9934	0.0101 / 0.0367
0.35	1.00	1.00	1.00	1.00	1.00	0.0312 / 0.0769
0.45	1.00	1.00	1.00	1.00	1.00	0.0502 / 0.1338

In some scenarios, it might be infeasible to get access to average representations for the target label. In this case, we propose a user-level defense whose ASR is also shown in the rightmost column. We observe that the ASR degrades gracefully, when switching to the user-level defense, a variant of our algorithm in which each user uploads the averaged representation over all samples rather than samples with the target label. Data homogeneity enables Algorithm 1 to distinguish malicious clients only based on averaged representations over all samples, without knowledge of the target label.

Table 2: ASR for CIFAR-10 under a continual learning setting shows the advantage of Algorithm 1.

$\alpha$	Noise Adding	Clipping and Noise Adding	RFA	G-SPECTRE	R-SPECTRE	Our Method
0.15	0.9212	0.9142	0.9353	0.8754	0.7575	0.0140
0.25	0.9177	0.9247	0.9528	0.9001	0.8826	0.0355
0.35	0.9388	0.9282	0.9563	0.9142	0.8932	0.0972
0.45	0.9207	0.9338	0.9598	0.9193	0.9091	0.1865

Compared with EMNIST dataset, CIFAR-10 is more difficult to learn. The smaller learning rate results in less effective early stopping and thus leads to slightly larger ASR in Table 2.

### 5.2 Ablation study: Main Task Accuracy (MTA) vs. Attack Success Rate (ASR) Tradeoff

Under homogeneous and static EMNIST dataset, we run an ablation study on one of the main components: the backbone network. Without the backbone network, our framework (in the one-shot setting) reduces to training baseline defenses with early stopping. Figure 3 shows the resulting achievable (ASR, MTA) as we tune the early-stopping round for  $\alpha = 0.45$ . Results for  $\alpha = 0.15$  are included in Appendix F.2. The curves start at the bottom left (0,0) and most of them first move up, learning the main tasks. Then, the curves veer to the right as the backdoor is learned. We want algorithms that achieve points close to the top left (0, 1).

Algorithm 1 achieves the green star (0.9967, 0.0502) when  $\alpha = 0.45$  (Figure 3). The blue curve (early stopping with no other defense) is far from (0, 1). This suggests that the backbone network and SPECTRE filtering are necessary to achieve the performance of Algorithm 1. The curve for early-stopped RFA (purple x’s) is also far from (0, 1) for large  $\alpha$ . Early-stopped R-SPECTRE without the backbone network (orange triangles) achieves a good MTA-ASR tradeoff (though still worse than that of Algorithm 1). However, we show in §5.3 that the MTA-ASR tradeoff of R-SPECTRE is significantly worse when clients’ data distribution changes dynamically. We observe similar trends for all baselines when  $\alpha = 0.15$  (Appendix F.2).

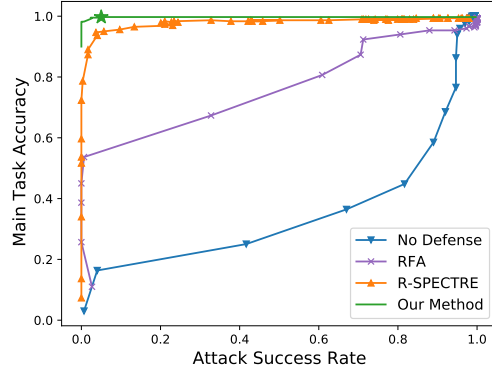


Figure 3: MTA-ASR tradeoff shows simple early stopping with no (other) defense far from the ideal (0,1) for  $\alpha = 0.45$ . R-SPECTRE with early stopping is more resilient, but all early-stopping-based prior defenses suffer when clients’ data changes dynamically as we show in §5.3. Algorithm 1 achieves close-to-ideal tradeoffs.

### 5.3 Defense under Time-varying Clients’ Data

We evaluate our defense in the dynamic setting, when the data distribution changes over time, for  $\alpha = 0.15$ . We compare Algorithm 1 with two variants: Periodic R-SPECTRE and our method using *only* shadow network prediction. Periodic R-SPECTRE is a direct extension of R-SPECTRE: the network is retrained from scratch with SPECTRE every  $R$  rounds, where  $R = 400$  is the interval of change in the client data. Next, we use the same training as our framework except the prediction only uses the shadow network (as opposed to using the backbone network as in Algorithm 1).

We set the data distribution varying period as 400 rounds and fix  $\alpha = 15\%$ . We use homogeneous EMNIST in the first phase  $e_1$ , then reduce the number of samples with labels 2-5 to 10% of the original in phase  $e_2$ , i.e., reduce the number of images with the label in  $\{2, 3, 4, 5\}$  from 10 to 1 for each client. Recall that the backdoor target label is 1. The MTA-ASR tradeoffs of all three algorithms in  $e_2$  are shown in Fig. 4 Results for additional periods and types of data distribution shift are shown in Appendix F.4.

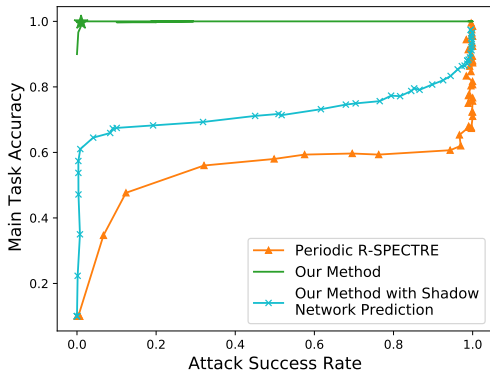


Figure 4: MTA-ASR Tradeoff with  $\alpha = 0.15$  after distribution shift (phase  $e_2$ ).

As we can see in Fig.4, adopting the early-stopping mechanism, Algorithm 1 achieves (0.9972, 0.0103) in phase  $e_2$ . However, the competing defenses suffer from the lack of training samples with labels 2-5. They take more time for the training accuracy to converge to 1, resulting in poor MTA-ASR tradeoffs. The backbone network in Algorithm 1 persists throughout the training, and is thus resilient to changes in data distributions; it achieves the point shown by a green star.

The MTA-ASR tradeoff of our method with shadow network prediction is better than that of periodic R-SPECTRE. The former conducts user filtering only after the convergence of backbone network  $N$  on label  $\ell$ , while the latter filters in every round. This indicates that filtering after  $N$  converges gives better performance.

### 5.4 Defense under Heterogeneous Dataset

We evaluate the ASR of Algorithm 1 and its two variants: sample-level and user-level defenses. In the sample level version, each user uploads the representations of samples with the target label without averaging, and the samples regarded as



backdoor images are filtered out. This is more complex and increases privacy concerns but is more robust against heterogeneous clients as shown in Table 3. On the other hand, user-level defense fails as heterogeneity of clients makes it challenging to detect corrupt users from user-level aggregate statistics. The label-level RFA and R-SPECTRE are evaluated after the network is trained for 1200 rounds. More experimental results are provided in Appendix F.3.

Table 3: ASR under EMNIST partitioned as the original data

$\alpha$	Label-level RFA	R-SPECTRE	Our Method with Sample-level Defense	Our Method	Our Method with User-level Defense
0.15	1.00	0.9967	0.0107	0.0307	0.5719
0.25	1.00	1.00	0.0166	0.0378	0.5912
0.35	1.00	1.00	0.0301	0.0836	0.6755
0.45	1.00	1.00	0.0534	0.1106	0.7359

## 6 Conclusion

Motivated by the success of robust covariance based filters in the non-FL setting, we propose a novel framework for defending against backdoor attacks in the federated continual learning setting. The main idea is to use such filters to reduce the fraction of corrupt model updates significantly, and then train an early stopped model (called a shadow model) on those filtered updates to get a clean model. This combination of filtering and early-stopping significantly improves upon existing defenses and we provide theoretical justifications of our approach. One of the main technical innovations is the parallel training of the backbone and the shadow models, which is critical for obtaining a reliable filter (via the backbone model) and a trustworthy predictor (via the shadow model).

## Acknowledgement

This material is based upon work supported by the National Science Foundation Convergence Accelerator grant CA-2040675, the U.S. Army Research Office and the U.S. Army Futures Command under Contract No. W911NF-20-D-0002, NSF grants CNS-2002664, IIS-1929955, DMS-2134012, CCF-2019844 as a part of NSF Institute for Foundations of Machine Learning (IFML), and CNS-2112471 as a part of NSF AI Institute for Future Edge Networks and Distributed Intelligence (AI-EDGE). The content of the information does not necessarily reflect the position or the policy of the government and no official endorsement should be inferred. This work was also supported in part by gift grants from J.P. Morgan Chase, Bosch, Siemens, Google, and Intel.

## References

- [1] Sana Awan, Bo Luo, and Fengjun Li. Contra: Defending against poisoning attacks in federated learning. In *European Symposium on Research in Computer Security*, pages 455–475. Springer, 2021.
- [2] Eugene Bagdasaryan, Andreas Veit, Yiqing Hua, Deborah Estrin, and Vitaly Shmatikov. How to backdoor federated learning. In *International Conference on Artificial Intelligence and Statistics*, pages 2938–2948. PMLR, 2020.
- [3] Mauro Barni, Kassem Kallas, and Benedetta Tondi. A new backdoor attack in cnns by training set corruption without label poisoning. In *2019 IEEE International Conference on Image Processing (ICIP)*, pages 101–105. IEEE, 2019.
- [4] Battista Biggio, Konrad Rieck, Davide Ariu, Christian Wressnegger, Iginio Corona, Giorgio Giacinto, and Fabio Roli. Poisoning behavioral malware clustering. In *Proceedings of the 2014 workshop on artificial intelligent and security workshop*, pages 27–36, 2014.
- [5] Peva Blanchard, Rachid Guerraoui, and Julien Stainer. Machine learning with adversaries: Byzantine tolerant gradient descent. In *Advances in Neural Information Processing Systems*, pages 119–129, 2017.
- [6] Xinyun Chen, Chang Liu, Bo Li, Kimberly Lu, and Dawn Song. Targeted backdoor attacks on deep learning systems using data poisoning. *arXiv preprint arXiv:1712.05526*, 2017.
- [7] Edward Chou, Florian Tramèr, Giancarlo Pellegrino, and Dan Boneh. Sentinet: Detecting physical attacks against deep learning systems. *arXiv preprint arXiv:1812.00292*, 2018.
- [8] Gregory Cohen, Saeed Afshar, Jonathan Tapson, and Andre Van Schaik. Emnist: Extending mnist to handwritten letters. In *2017 international joint conference on neural networks (IJCNN)*, pages 2921–2926. IEEE, 2017.

- [9] Chandler Davis and William Morton Kahan. The rotation of eigenvectors by a perturbation. iii. *SIAM Journal on Numerical Analysis*, 7(1):1–46, 1970.
- [10] Ilias Diakonikolas, Gautam Kamath, Daniel Kane, Jerry Li, Ankur Moitra, and Alistair Stewart. Robust estimators in high-dimensions without the computational intractability. *SIAM Journal on Computing*, 48(2):742–864, 2019.
- [11] Ilias Diakonikolas, Gautam Kamath, Daniel M Kane, Jerry Li, Ankur Moitra, and Alistair Stewart. Being robust (in high dimensions) can be practical. In *International Conference on Machine Learning*, pages 999–1008. PMLR, 2017.
- [12] Tianyu Gu, Brendan Dolan-Gavitt, and Siddharth Garg. Badnets: Identifying vulnerabilities in the machine learning model supply chain. *arXiv preprint arXiv:1708.06733*, 2017.
- [13] Jonathan Hayase, Weihao Kong, Raghav Somani, and Sewoong Oh. SPECTRE: Defending against backdoor attacks using robust statistics. In *International Conference on Machine Learning*, pages 4129–4139. PMLR, 2021.
- [14] Kaiming He, Xiangyu Zhang, Shaoqing Ren, and Jian Sun. Deep residual learning for image recognition. In *Proceedings of the IEEE conference on computer vision and pattern recognition*, pages 770–778, 2016.
- [15] Peter J Huber. Robust estimation of a location parameter. In *Breakthroughs in statistics*, pages 492–518. Springer, 1992.
- [16] Andrew Ilyas, Shibani Santurkar, Dimitris Tsipras, Logan Engstrom, Brandon Tran, and Aleksander Madry. Adversarial examples are not bugs, they are features. In *Advances in Neural Information Processing Systems*, pages 125–136, 2019.
- [17] Jakub Konečný, H Brendan McMahan, Daniel Ramage, and Peter Richtárik. Federated optimization: Distributed machine learning for on-device intelligence. *arXiv preprint arXiv:1610.02527*, 2016.
- [18] Alex Krizhevsky, Geoffrey Hinton, et al. Learning multiple layers of features from tiny images. 2009.
- [19] Pavel Laskov. Practical evasion of a learning-based classifier: A case study. In *2014 IEEE symposium on security and privacy*, pages 197–211. IEEE, 2014.
- [20] Kimin Lee, Kibok Lee, Honglak Lee, and Jinwoo Shin. A simple unified framework for detecting out-of-distribution samples and adversarial attacks. In *Advances in Neural Information Processing Systems*, pages 7167–7177, 2018.
- [21] Mingchen Li, Mahdi Soltanolkotabi, and Samet Oymak. Gradient descent with early stopping is provably robust to label noise for overparameterized neural networks. In *International conference on artificial intelligence and statistics*, pages 4313–4324. PMLR, 2020.
- [22] Shaofeng Li, Minhui Xue, Benjamin Zi Hao Zhao, Haojin Zhu, and Xinpeng Zhang. Invisible backdoor attacks on deep neural networks via steganography and regularization. *arXiv preprint arXiv:1909.02742*, 2019.
- [23] Yige Li, Xixiang Lyu, Nodens Koren, Lingjuan Lyu, Bo Li, and Xingjun Ma. Anti-backdoor learning: Training clean models on poisoned data. *Advances in Neural Information Processing Systems*, 34, 2021.
- [24] Yige Li, Xixiang Lyu, Nodens Koren, Lingjuan Lyu, Bo Li, and Xingjun Ma. Neural attention distillation: Erasing backdoor triggers from deep neural networks. *arXiv preprint arXiv:2101.05930*, 2021.
- [25] Shiyu Liang, Yixuan Li, and Rayadurgam Srikant. Enhancing the reliability of out-of-distribution image detection in neural networks. *arXiv preprint arXiv:1706.02690*, 2017.
- [26] Jing Liu, Chulin Xie, Krishnaram Kenthapadi, Oluwasanmi O Koyejo, and Bo Li. Rvfr: Robust vertical federated learning via feature subspace recovery. 2021.
- [27] Kang Liu, Brendan Dolan-Gavitt, and Siddharth Garg. Fine-pruning: Defending against backdooring attacks on deep neural networks. In *International Symposium on Research in Attacks, Intrusions, and Defenses*, pages 273–294. Springer, 2018.
- [28] Yingqi Liu, Shiqing Ma, Yousra Aafer, Wen-Chuan Lee, Juan Zhai, Weihang Wang, and Xiangyu Zhang. Trojaning attack on neural networks. 2017.
- [29] Yunfei Liu, Xingjun Ma, James Bailey, and Feng Lu. Reflection backdoor: A natural backdoor attack on deep neural networks. In *European Conference on Computer Vision*, pages 182–199. Springer, 2020.
- [30] Aleksander Madry, Aleksandar Makelov, Ludwig Schmidt, Dimitris Tsipras, and Adrian Vladu. Towards deep learning models resistant to adversarial attacks. *arXiv preprint arXiv:1706.06083*, 2017.
- [31] Krishna Pillutla, Sham M Kakade, and Zaid Harchaoui. Robust aggregation for federated learning. *arXiv preprint arXiv:1912.13445*, 2019.

- [32] Stefano Savazzi, Monica Nicoli, Mehdi Bennis, Sanaz Kianoush, and Luca Barbieri. Opportunities of federated learning in connected, cooperative, and automated industrial systems. *IEEE Communications Magazine*, 59(2):16–21, 2021.
- [33] Jacob Steinhardt, Pang Wei W Koh, and Percy S Liang. Certified defenses for data poisoning attacks. In *Advances in neural information processing systems*, pages 3517–3529, 2017.
- [34] Ziteng Sun, Peter Kairouz, Ananda Theertha Suresh, and H Brendan McMahan. Can you really backdoor federated learning? *arXiv preprint arXiv:1911.07963*, 2019.
- [35] Vale Tolpegin, Stacey Truex, Mehmet Emre Gursoy, and Ling Liu. Data poisoning attacks against federated learning systems. In *European Symposium on Research in Computer Security*, pages 480–501. Springer, 2020.
- [36] Brandon Tran, Jerry Li, and Aleksander Madry. Spectral signatures in backdoor attacks. *Advances in neural information processing systems*, 31, 2018.
- [37] Binghui Wang, Xiaoyu Cao, and Neil Zhenqiang Gong. On certifying robustness against backdoor attacks via randomized smoothing. *arXiv preprint arXiv:2002.11750*, 2020.
- [38] Bolun Wang, Yuanshun Yao, Shawn Shan, Huiying Li, Bimal Viswanath, Haitao Zheng, and Ben Y Zhao. Neural cleanse: Identifying and mitigating backdoor attacks in neural networks. In *2019 IEEE Symposium on Security and Privacy (SP)*, pages 707–723. IEEE, 2019.
- [39] Maurice Weber, Xiaojun Xu, Bojan Karlas, Ce Zhang, and Bo Li. Rab: Provable robustness against backdoor attacks. *arXiv preprint arXiv:2003.08904*, 2020.
- [40] Chulin Xie, Minghao Chen, Pin-Yu Chen, and Bo Li. Crfl: Certifiably robust federated learning against backdoor attacks. In *International Conference on Machine Learning*, pages 11372–11382. PMLR, 2021.
- [41] Chaofei Yang, Qing Wu, Hai Li, and Yiran Chen. Generative poisoning attack method against neural networks. *arXiv preprint arXiv:1703.01340*, 2017.
- [42] Haoti Zhong, Cong Liao, Anna Cinzia Squicciarini, Sencun Zhu, and David Miller. Backdoor embedding in convolutional neural network models via invisible perturbation. In *Proceedings of the Tenth ACM Conference on Data and Application Security and Privacy*, pages 97–108, 2020.

## Appendix

### A Ethical Considerations

This paper studies defenses against backdoor attacks in FL pipelines. The main ethical implications are surrounding the evaluation of our defense. To demonstrate robustness against a backdoor attack, we would ideally like to deploy our methods in a real ML pipeline and demonstrate that our method can defend against real-world backdoor attacks. However, this is infeasible due both to constraints in deploying new user-facing FL technologies and in the relative rarity of known backdoor attacks in the wild. To deal with these constraints, we evaluated our methods on benchmark datasets and backdoor attacks introduced by us. While this evaluation setup is less realistic than a real FL pipeline, it also avoids possible ethical issues if one were to deploy a defense that fails in a safety-critical situation. That is, although our approach has very low ASR, it is not zero. In some cases, an attacker might be able to launch severe attacks if they can manage to backdoor even a single sample at test time. Such scenarios are likely ill-suited to purely statistical defenses like ours.

### B Related Work

**Backdoor attacks.** There has been a vast body of attacks on machine learning (ML) pipelines. In this work, we consider only *training-time* attacks, in which the attacker modifies either the training data or process to meet their goals. Inference-time attacks are discussed in several survey papers [30, 16]. Further, we do not consider data poisoning attacks, in which the goal of the adversary is simply to decrease the model’s prediction accuracy [41, 4] which has also been studied in the federated setting [34]. Instead, we focus on *backdoor attacks*, where the attacker’s goal is to train a model to output a target classification label on samples that contain a trigger signal (specified by the attacker) while classify other samples correctly at test-time [12]. The most commonly-studied backdoor attack is a *pixel attack*, in which the attacker inserts a small pattern of pixels into a subset of training samples of a given source class, and changes their labels to the target label [12]. Pixel attacks can be effective even when only a small fraction of training data is corrupted [12]. Many subsequent works have explored other types of backdoor attacks, including (but not limited to) periodic signals [42], feature-space perturbations [6, 28], reflections [29], human-imperceptible perturbations [22], and FL model replacement that explicitly try to evade anomaly detection [2]. Although our evaluation will focus on pixel attacks, our experiments suggest that our insights translate to other types of attacks as well (Appendix F.5 and F.6).

**Backdoor defenses.** As mentioned earlier, many backdoor defenses can be viewed as taking one (or more) of three approaches: (1) Malicious data detection, (2) Robust training, and (3) Trigger identification.

Malicious data detection-based methods exploit the idea that adversarial samples will differ from the benign data distribution (e.g., they may be outliers). Many such defenses require access to clean samples [25, 20, 33], which we assume to be unavailable. Others work only when the initial adversarial fraction is large, as in anti-backdoor learning [23] (see § 3.2), or small, as in robust vertical FL [26]; we instead require a method that works across all adversarial fractions. Recently, *SPECTRE* proposed using robust covariance estimation to estimate the covariance of the benign data from a (partially-corrupted) dataset [13]. The data samples are whitened to amplify the spectral signature of corrupted data. Malicious samples are then filtered out by thresholding based on a *QUantum Entropy (QUE)* score, which projects the whitened data down to a scalar. We use *SPECTRE* as a building block of our algorithm, and also as a baseline for comparison. To adapt *SPECTRE* to the FL setting, we apply it to gradients (we call this G-*SPECTRE*) or sample representations (R-*SPECTRE*), each averaged over a single client’s local data with target label  $\ell$ . However, we see in § 3.1 that *SPECTRE* alone does not work in the continuous learning setting.

Robust training methods do not explicitly identify and/or filter outliers; instead, they modify the training (and/or testing) procedure to implicitly remove their contribution. For example, *Robust Federated Aggregation (RFA)* provides a robust secure aggregation oracle based on the geometric median [31]. It is shown to be robust against data poisoning attacks both theoretically and empirically. However, it was not evaluated on backdoor attacks. In this work, we adopt RFA as a baseline, and show that it too suffers from backdoor leakage (§ 3.1). Other variants of robust training methods require a known bound on the magnitude of the adversarial perturbation; for example, randomized smoothing [37, 39] ensures that the classifier outputs the same label for all points within a ball centered at a particular sample. We assume the radius of adversarial perturbations to be unknown at training time. Other approaches again require access to clean data, which we assume to be unavailable. Examples include fine-pruning [27], which trains a pruned, fine-tuned model from clean data.

Trigger identification approaches typically examine the training data to infer the structure of a trigger. For example, NeuralCleanse [38] searches for data perturbations that change the classification of a sample to a target class. SentiNet [7] uses techniques from model interpretability to identify contiguous, salient regions of input images. These approaches are ill-suited to the FL setting, as they require fine-grained access to training samples and are often tailored to a specific type of backdoor trigger (e.g., pixel attacks).

Finally, note that there is a large body of work defending against data poisoning attacks [34, 31, 5, 1, 19, 35]. In general, such defenses do not work against backdoor attacks. For example, we show in § 3.1 and § 5 that defenses against data poisoning attacks such as RFA [31], norm clipping [34], and noise addition [34] are ineffective against backdoor attacks, particularly in the continual learning setting.

## C Complete proofs of the main theoretical results

We provide proofs of main results and accompanying technical lemmas. We use  $c, c', C, C', \dots$  to denote generic numerical constants that might differ from line to line.

### C.1 Proof of Theorem 1

The proof proceeds in two steps. First, we show that under Assumption 1, the direction of the top eigenvector of the empirical covariance is aligned with the direction of the center of the poisoned representations (Lemma C.1). We next show that filtering with the quantum score significantly reduces the number of poisoned clients (Lemma C.2).

We let  $\hat{\Sigma}$  be the output of the robust covariance estimator in Algorithm 2. After whitening by  $\hat{\Sigma}^{-1/2}$ , we let  $\tilde{\Sigma}_c = \hat{\Sigma}^{-1/2} \Sigma_c \hat{\Sigma}^{-1/2}$ ,  $\tilde{\Sigma}_p = \hat{\Sigma}^{-1/2} \Sigma_p \hat{\Sigma}^{-1/2}$ ,  $\tilde{\Delta} = \hat{\Sigma}^{-1/2} \Delta$ ,  $\tilde{\mu}_p = \hat{\Sigma}^{-1/2} \mu_p$ , and  $\tilde{\mu}_c = \hat{\Sigma}^{-1/2} \mu_c$ .

The next lemma shows that as we have a larger separation  $\|\tilde{\Delta}\|$ , we get a better estimate of the direction of the poisons,  $\tilde{\Delta}/\|\tilde{\Delta}\|$ , using the principal component,  $v$ , of the whitened representations  $S' = \{\Sigma^{-1/2}(h_i - \mu)\}_{i=1}^{n_r}$ . The estimation error is measured in  $\sin^2$  of the angle between the two.

**Lemma C.1** (Estimating  $\tilde{\Delta}$  with top eigenvector). *Under the assumptions of Theorem 1,*

$$\sin^2(v, \tilde{\Delta}/\|\tilde{\Delta}\|) = 1 - (v^T \tilde{\Delta}/\|\tilde{\Delta}\|)^2 \leq c \frac{(\log(1/\alpha) + \xi)^2}{\|\tilde{\Delta}\|^4}. \quad (1)$$

We next show that when projected onto any direction  $v$ , the number of corrupted client updates passing the filter is determined by how closely aligned  $v$  is with the direction of the poisoned data,  $\tilde{\Delta}$ , and the magnitude of the separation,  $\|\tilde{\Delta}\|$ .

**Lemma C.2** (Quantum score filtering). *Under the hypotheses of Theorem 1,*

$$\frac{|S_{\text{poison}} \setminus S_{\text{filter}}|}{|(S_{\text{poison}} \cup S_{\text{clean}}) \setminus S_{\text{filter}}|} \leq c' \alpha n_r Q\left(\frac{v^T \tilde{\Delta} - c\sqrt{\log(1/\alpha)}}{\xi^{1/2}}\right), \quad (2)$$

where  $Q(t) = \int_t^\infty (1/\sqrt{2\pi})e^{-\frac{x^2}{2}} dx$  is the tail of the standard Gaussian.

Since  $\|\tilde{\Delta}\|^2 \geq C(\log(1/\alpha) + \xi)$ , Lemma C.1 implies  $v^T \tilde{\Delta} \geq (1/2)\|\tilde{\Delta}\|$ . Since  $(v^T \tilde{\Delta} - c\sqrt{\log(1/\alpha)})/\xi^{1/2} \geq C'\sqrt{\log(1/\alpha)}/\xi$ , Lemma C.2 implies that  $|S_{\text{poison}} \setminus S_{\text{filter}}| \leq \alpha^{C''/\xi}$ . Since  $\xi < 1$ , we can make any desired exponent by increasing the separation by a constant factor.

### C.1.1 Proof of Lemma C.1

Let  $\tilde{\Sigma}$  denote the empirical covariance of the whitened representations. With a large enough sample size, we have the following bound on the robustly estimated covariance.

**Theorem 2** (Robust covariance estimation [11, Theorem 3.3]). *If the sample size is  $n_r = \Omega((d^2/\alpha^2)\text{polylog}(d/\alpha))$  with a large enough constant then with probability 9/10,*

$$\|\hat{\Sigma}^{-1/2}\Sigma_c\hat{\Sigma}^{-1/2} - \mathbf{I}_d\|_F \leq c\alpha \log(1/\alpha), \quad (3)$$

for some universal constant  $c > 0$  where  $\|A\|_F$  denotes the Frobenius norm of a matrix  $A$ .

Denoting  $\tilde{\Sigma} = \hat{\Sigma}^{-1/2}\Sigma_{\text{emp}}\hat{\Sigma}^{-1/2}$  with the empirical covariance of the clean representations denoted by  $\Sigma_{\text{emp}} = (1/n)\sum_{i=1}^n (h_i - \mu_{\text{emp}})(h_i - \mu_{\text{emp}})^T = (1-\alpha)\hat{\Sigma}_c + \alpha\hat{\Sigma}_p + \alpha(1-\alpha)\hat{\Delta}\hat{\Delta}^T$ , where  $\hat{\Sigma}_c$ ,  $\hat{\Sigma}_p$ , and  $\hat{\Delta}$  are the empirical counterparts, we can use this to bound,

$$\begin{aligned} & \|\tilde{\Sigma} - (1-\alpha)\mathbf{I}_d - \alpha\hat{\Sigma}_p - \alpha(1-\alpha)\tilde{\Delta}\tilde{\Delta}^T\| \\ & \leq (1-\alpha)\|\hat{\Sigma}^{-1/2}(\hat{\Sigma}_c - \Sigma_c)\hat{\Sigma}^{-1/2}\| + (1-\alpha)\|\hat{\Sigma}^{-1/2}\Sigma_c\hat{\Sigma}^{-1/2} - \mathbf{I}_d\| \\ & \quad + \alpha\|\hat{\Sigma}^{-1/2}(\Sigma_p - \hat{\Sigma}_p)\hat{\Sigma}^{-1/2}\| + \alpha(1-\alpha)\|\hat{\Sigma}^{-1/2}(\Delta\Delta^T - \hat{\Delta}\hat{\Delta}^T)\hat{\Sigma}^{-1/2}\| \\ & \leq c'\alpha \log(1/\alpha), \end{aligned} \quad (4)$$

for a large enough sample size  $n_r = \tilde{\Omega}(d^2/\alpha^3)$ . Among other things, this implies that

$$\|\tilde{\Sigma} - (1-\alpha)\mathbf{I}\| \geq \alpha(1-\alpha)\|\tilde{\Delta}\|^2 - c'\alpha \log(1/\alpha). \quad (5)$$

We use Davis-Kahan theorem to turn a spectral norm bound between two matrices into an angular distance bound between the top singular vectors of the two matrices:

$$\begin{aligned} \sqrt{1 - \frac{(v^T \tilde{\Delta})^2}{\|\tilde{\Delta}\|^2}} & \leq \frac{\|(\|\tilde{\Sigma}\| - (1-\alpha))vv^T - \alpha(1-\alpha)\tilde{\Delta}\tilde{\Delta}^T\|_F}{\|\tilde{\Sigma} - (1-\alpha)\mathbf{I}\|} \\ & \leq \frac{\sqrt{2}\|(\|\tilde{\Sigma}\| - (1-\alpha))vv^T - \alpha(1-\alpha)\tilde{\Delta}\tilde{\Delta}^T\|}{\|\tilde{\Sigma} - (1-\alpha)\mathbf{I}\|} \\ & \leq \frac{2\sqrt{2}\|\tilde{\Sigma} - (1-\alpha)\mathbf{I} - \alpha(1-\alpha)\tilde{\Delta}\tilde{\Delta}^T\|}{\|\tilde{\Sigma} - (1-\alpha)\mathbf{I}\|} \\ & \leq \frac{c\alpha(\log(1/\alpha) + \|\tilde{\Sigma}_p\|)}{\alpha(1-\alpha)\|\tilde{\Delta}\|^2 - c'\alpha \log(1/\alpha)}, \end{aligned} \quad (6)$$

where  $\|A\|$  and  $\|A\|_F$  denote spectral and Frobenius norms of a matrix  $A$ , respectively, the first inequality follows from Davis-Kahan theorem [9], the second inequality follows from the fact that Frobenius norm of a rank-2 matrix is bounded by  $\sqrt{2}$  times the spectral norm, and the third inequality follows from the fact that  $(\|\tilde{\Sigma}\| - (1-\alpha))vv^T$  is the best rank one approximation of  $\tilde{\Sigma} - (1-\alpha)\mathbf{I}$  and hence  $\|(\|\tilde{\Sigma}\| - (1-\alpha))vv^T - \tilde{\Delta}\tilde{\Delta}^T\| \leq \|(\|\tilde{\Sigma}\| - (1-\alpha))vv^T - (\tilde{\Sigma} - (1-\alpha)\mathbf{I})\| + \|(\tilde{\Sigma} - (1-\alpha)\mathbf{I}) - \tilde{\Delta}\tilde{\Delta}^T\| \leq 2\|\tilde{\Sigma} - (1-\alpha)\mathbf{I} - \tilde{\Delta}\tilde{\Delta}^T\|$ . The last inequality follows from Eq. (4) and Eq. (5). For  $\alpha \leq 1/2$  and  $\|\tilde{\Delta}\| \geq \sqrt{\log(1/\alpha)}$ , this implies the desired result.

### C.1.2 Proof of Lemma C.2

We consider a scenario where the QUEscore of a (whitened and centered) representation  $\tilde{h}_i = \hat{\Sigma}^{-1/2}(h_i - \hat{\mu}_c)$ , where  $\hat{\mu}_c$  is the robust estimate of  $\mu_c$ , is computed as

$$\tau_i^{(\beta)} = \frac{\tilde{h}_i^T Q_\beta \tilde{h}_i}{\text{Tr}(Q_\beta)}, \quad (7)$$

where  $Q_\beta = \exp((\alpha/\|\tilde{\Sigma}\| - 1)(\tilde{\Sigma} - \mathbf{I}))$ . We analyze the case where we choose  $\beta = \infty$ , such that  $\tau_i^{(\infty)} = (v^T \tilde{h}_i)^2$  and the threshold  $T$  returned by SPECTRE satisfies the following. If we have infinite samples and there is no error in the estimates  $v$ ,  $\tilde{\Sigma}$ , and  $\hat{\mu}_c$ , then we have  $Q^{-1}((3/4)\alpha) \leq T^{1/2} \leq Q^{-1}((1/4)\alpha)$ , which follows from the fact that for the clean data with identity covariance, we can filter out at most  $1.5\alpha$  fraction of the data (which happens if we do not filter out any of the poisoned data points) and we can filter out at least  $0.5\alpha$  fraction of the data (which happens if we filter out all the poisoned data). With finite samples and estimation errors in the robust estimates, we get the following:

$$Q^{-1}((3/4)\alpha + \alpha^2/d) - c'\alpha/d \leq T^{1/2} \leq Q^{-1}((1/4)\alpha - c'\alpha^2/d) + c'\alpha/d, \quad (8)$$

where  $Q(\cdot)$  is the tail of a standard Gaussian as defined in Lemma C.2 and we used the fact that for a large enough sample size we have  $\|v^T \hat{\Sigma}^{-1/2}(\mu_c - \hat{\mu}_c)\| \leq c'\alpha/d$ .

At test time, when we filter out data points with QUEscore larger than  $T$ , we have that we filter out at most clean  $|S_{\text{clean}} \cap S_{\text{filter}}| \leq 2\alpha n_r$  representations for a large enough  $d$ . Similarly, we are guaranteed that the remaining poisoned representations are at most  $|S_{\text{poison}} \setminus S_{\text{filter}}| \leq Q((v^T \tilde{\Delta} - T^{1/2})/\xi^{1/2})(\alpha n_r)$ . Since from above bound  $T^{1/2} \leq c\sqrt{\log(1/\alpha)}$ , this proves the desired bound.

## C.2 Assumptions for Corollary 4.1

Corollary 4.1 follows as a corollary of [21, Theorem 2.2]. This critically relies on an assumption on a  $(\varepsilon_0, M)$ -clusterable dataset  $\{(x_i \in \mathbb{R}^{d_0}, y_i \in \mathbb{R})\}_{i=1}^{n_r}$  and overparametrized two-layer neural network models, as defined in Assumption 2 below.

**Assumption 2** ( $(\alpha, n_r, \varepsilon_0, \varepsilon_1, M, L, \hat{M}, C, \lambda, W)$ -model). *The  $(1 - \alpha)$  fraction of data points are clean and originate from  $M$  clusters with each cluster containing  $n_r/M$  data points. Cluster centers are unit norm vectors,  $\{\mu_q \in \mathbb{R}^{d_0}\}_{q=1}^M$ . An input  $x_i$  that belong to the  $q$ -th cluster obeys  $\|x_i - \mu_q\| \leq \varepsilon_0$ , with  $\varepsilon_0$  denoting the input noise level. The labels  $y$  belong to one of the  $L$  classes and we place them evenly in  $[-1, 1]$  in the training such that labels correspond to  $y \in \{-1, -1 + 1/(L-1), \dots, 1\}$ . We let  $C = [\mu_1, \dots, \mu_M]^T \in \mathbb{R}^{M \times d_0}$  and define  $\lambda = \lambda(C)$  as the minimum eigenvalue of the matrix  $CC^T \odot \mathbb{E}[\phi'(Cg)\phi'(Cg)^T]$  for  $g \sim \mathcal{N}(0, \mathbf{I}_{d_0})$ .*

*All clean data points in the same cluster share the same label. Any two clusters obey  $|\mu_q - \mu_{q'}| \geq 2\varepsilon_0 + \varepsilon_1$ , where  $\varepsilon_1$  is the size of the trigger. The corrupted data points are generated from a data point  $x_i$  with a source label  $y_i = y_{\text{source}}$  belonging to one of the clusters for the source. A fixed trigger  $\delta$  is added to the input and labelled as a target label  $q$  such that the corrupted paired example is  $(x_i + \delta, q)$ . We train on the combined dataset with  $\alpha n_r$  corrupted points and  $(1 - \alpha)n_r$  uncorrupted points. We train a neural network of the form  $f_W(x) = v^T \phi(Wx)$  for a trainable parameter  $W \in \mathbb{R}^{\hat{M} \times d_0}$  and a fixed  $v \in \mathbb{R}^{\hat{M}}$ , where the head  $v$  is fixed as  $1/\sqrt{\hat{M}}$  for half of the entries and  $-1/\sqrt{\hat{M}}$  for the other half. We assume the activation function  $\phi: \mathbb{R} \rightarrow \mathbb{R}$  satisfy  $|\phi'(z)|, |\phi''(z)| < c'$  for some constant  $c' > 0$ .*

## C.3 Necessity of robust covariance estimation

To highlight that SPECTRE, and the robust covariance estimation, is critical in achieving this guarantee, we next show that under the same assumptions, using the QUEscore filtering without whitening fails and also using whitening with non-robust covariance estimation also fails, in the sense that the fraction of the corrupted data is non-decreasing. We construct an example within Assumption 1 as follows:  $\mu_c = 0$  and  $\Sigma_c = \sigma^2(\mathbf{I} - (1 - \delta)uu^T)$  for a unit norm  $u$ . We place all the poisons at  $\mu_p = au$  with  $\xi = 0$  and covariance  $\Sigma_p$  zero. We let  $\delta \leq a/(c_m^2 \log(1/\alpha))$  such that the separation condition is met. By increasing  $\sigma^2$ , we can make the inner product of top PCA direction  $v_{\text{combined}}$  of the combined data and the direction of the poisons  $u$  arbitrarily small. Hence, after finding the threshold  $T$  in the projected representations  $v_{\text{combined}}^T h_i$  and using this to filter out the representations, as proposed in [36], the ratio of the poisons can only increase as all the poisons are placed close to the center of the clean representations after projection. The same construction and conclusion holds for the case when we whitened with not the robustly estimated covariance, but the QUEscore based filter with  $\beta = \infty$  projects data first onto the PCA direction of the whitened data, which can be made arbitrarily orthogonal to the direction of the poisons, in high dimensions, i.e.  $v_{\text{whitened}}^T u \leq 2/d$  with high probability. This follows from the fact that after (non-robust) whitening, all directions are equivalent and the chance of PCA finding the direction of the poisons is uniformly at random over all directions in the  $d$  dimensional space.

## D Algorithm Details

In the client filtering process, the collected representations are projected down to a  $k$ -dimensional space by  $U$ , then whitened to get  $\tilde{\mathbf{h}}_j = \hat{\Sigma}^{-1/2}(\mathbf{U}^T \mathbf{h}_j - \hat{\boldsymbol{\mu}}) \in \mathbb{R}^k$  for all  $j \in \mathcal{C}_r$ . The projection onto  $U$  is to reduce computational complexity, which is less critical for the performance of the filter. The whitening with clean covariance  $\hat{\Sigma}$  and clean mean  $\hat{\boldsymbol{\mu}}$  ensures that the poisoned representations stand out from the clean ones and is critical for the performance of the filter. Based on the whitened representations, the server calculates QUE scores (which roughly translates as the scaled-norm of the whitened representation) for all clients and keeps the clients with scores less than the threshold  $T$  as  $\mathcal{C}'_r$  (FILTER in line 15). The details of GETTHRESHOLD and the client filtering process, FILTER, are shown in Algorithms 2 and 3.

---

### Algorithm 2: GETTHRESHOLD

---

**input** : representation  $S = \{\mathbf{h}_i\}_{i=1}^n$ , malicious rate upper bound  $\bar{\alpha}$ , dimension  $k$ , QUE parameter  $\beta$ .

$$\boldsymbol{\mu}(S) \leftarrow \frac{1}{n} \sum_{i=1}^n \mathbf{h}_i;$$

$$S_1 = \{\mathbf{h}_i - \boldsymbol{\mu}(S)\}_{i=1}^n;$$

$$\mathbf{V}, \boldsymbol{\Lambda}, \mathbf{U} = \text{SVD}_k(S_1);$$

$$S_2 \leftarrow \{\mathbf{U}^T \mathbf{h}_i\}_{\mathbf{h}_i \in S};$$

$$\hat{\Sigma}, \hat{\boldsymbol{\mu}} \leftarrow \text{ROBUSTEST}(S_2, \bar{\alpha}); [10]$$

$$S_3 \leftarrow \left\{ \hat{\Sigma}^{-1/2} (\bar{\mathbf{h}}_i - \hat{\boldsymbol{\mu}}) \right\}_{\bar{\mathbf{h}}_i \in S_2};$$

$$\{t_i\}_{i=1}^n \leftarrow \text{QUESCORE}(S_3, \beta)$$

[Algorithm 4]

$$T \leftarrow \text{the } 1.5\bar{\alpha}n\text{-th largest value in } \{t_i\}_{i=1}^n;$$

**return**  $\hat{\Sigma}, \hat{\boldsymbol{\mu}}, T, U$

---



---

### Algorithm 3: FILTER

---

**input** :  $S = \{\bar{\mathbf{h}}_i \in \mathbb{R}^k\}_{i=1}^n$ , estimated covariance  $\hat{\Sigma}$ , estimated mean  $\hat{\boldsymbol{\mu}}$ , threshold  $T$ , QUE parameter  $\beta$ .

$$S' \leftarrow \left\{ \hat{\Sigma}^{-1/2} (\bar{\mathbf{h}}_i - \hat{\boldsymbol{\mu}}) \right\}_{\bar{\mathbf{h}}_i \in S};$$

$$\{t_i\} \leftarrow \text{QUESCORE}(S', \beta)$$

[Algorithm 4]

**return** clients with QUE-scores smaller than  $T$

---

The details of the QUESCORE[13] is shown in Algorithm 4

---

### Algorithm 4: QUESCORE [13]

---

**input** :  $S = \{\tilde{\mathbf{h}}_i \in \mathbb{R}^k\}_{i=1}^n$ , QUE parameter  $\beta$ .

$$t_i \leftarrow \frac{\tilde{\mathbf{h}}_i^\top Q_\beta \tilde{\mathbf{h}}_i}{\text{Tr}(Q_\beta)}, \quad \forall i \in [n],$$

where  $Q_\beta = \exp\left(\frac{\beta(\tilde{\Sigma} - \mathbf{I})}{\|\tilde{\Sigma}\|_2 - 1}\right)$  and  $\tilde{\Sigma} = \frac{1}{n} \sum_{i=1}^n \tilde{\mathbf{h}}_i \tilde{\mathbf{h}}_i^\top$ .

**return**  $\{t_i\}_{i=1}^n$

---

## E Experimental Details

In the experiments in §5, we train on the EMNIST and CIFAR-10 datasets. In the EMNIST dataset, there are 3383 users with roughly 100 images in ten labels per user with heterogeneous label distributions. We train a convolutional network with two convolutional layers, max-pooling, dropout, and two dense layers. The CIFAR-10 dataset has 50,000 training examples, with 5000 samples in each label. We partition those samples to 500 users uniformly at random and train a ResNet-18 [14].

For both datasets, the server randomly selects 50 clients each round, and each client trains the current model with the local data with batch size 20, learning rate 0.1, and for two iterations. The server learning rate is 0.5. The attacker tries to make 7’s predicted as 1’s for EMNIST and horses as automobiles for CIFAR-10. The backdoor trigger is a  $5 \times 5$ -pixel black square at the bottom right corner of the image. An  $\alpha$  fraction of the clients are chosen to be malicious, who are given 10 corrupted samples. We set the malicious rate  $\alpha$  as its upper bound, i.e.,  $\alpha = \bar{\alpha}$ . We study first homogeneous and static settings, and we discuss heterogeneous and dynamic settings in §5.4 and §5.3. In our framework, we set the retraining threshold  $\epsilon_1$  as 2%, and the convergence threshold  $\epsilon_2$  as 0.05%. We let the dimensionality reduction parameter  $k$  be 32 and set the QUE parameter  $\beta$  as 4 in Algorithm 1.

**Baselines.** SPECTRE [13] adopts robust covariance estimation and data whitening to amplify the spectral signature of corrupted data, and then detects backdoor samples based on quantum entropy (QUE) score. In federated learning settings, we adopt gradient- and representation-based SPECTRE, which takes as input the gradient updates or sample representations averaged over a single client’s local data with target label  $\ell$ . For both versions, we conduct the robust estimation and quantum score filtering every training round regardless of the computation constraints. We let the dimensionality reduction parameter  $k$  be 32 and set the QUE parameter  $\beta$  as 4.

RFA [31] provides a robust secure aggregation oracle based on the geometric median, which is calculated by the Weiszfeld’s Algorithm. In our experiments, we implement RFA with 4-iteration Weiszfeld’s Algorithm. We also consider the label-level RFA: for each label, the geometric median of the aggregated gradient uploaded from each client is estimated. The server then updates the model based on the averaged geometric medians of all labels.

Norm Clipping defense [34] bounds the norm of each model update to at most some threshold  $M$ , and Noise Adding method [34] is to add a small amount of Gaussian noise to the updates. In our experiments, we set the norm threshold  $M$  as 3 and add independent Gaussian noise with variance 0.03 to each coordinate.

### E.0.1 Resource Costs

All algorithms including ours are implemented and performed on a server with two Xeon Processor E5-2680 CPUs. Running all defenses for our experiments took approximately 1000 CPU-core hours.

## F Additional experimental results

### F.1 Backdoor Leakage under CIFAR-10

Under the CIFAR-10 dataset, we show that *backdoor leakage* phenomenon also results in the failure of existing backdoor defenses in Figure 5. Similar to Figure 1(a), we fix the malicious rate as  $\alpha = 3\%$  and run the experiments for 12,000 training rounds under the static setting where data distribution is fixed over time. We can observe that the attack success rate (ASR) of all competing defenses eventually approach near 1, while the ASR of our algorithm keeps near 0 (0.0092) all the time.

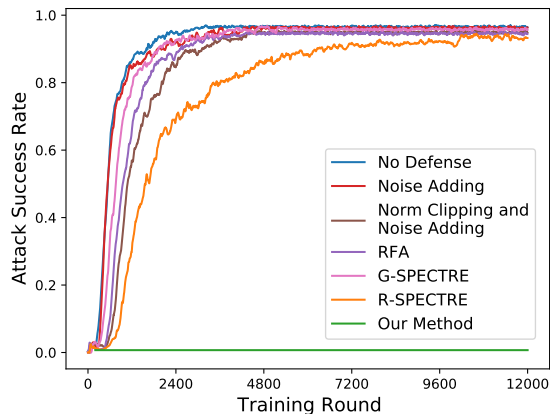


Figure 5: Backdoor leakage causes competing defenses to fail eventually under CIFAR-10, even with a small  $\alpha = 3\%$ .



## F.2 MTA-ASR Tradeoffs

We include the MTA-ASR tradeoff plot in Figure 6. The experimental setup is identical to Figure 3, except we take  $\alpha = 0.15$ .

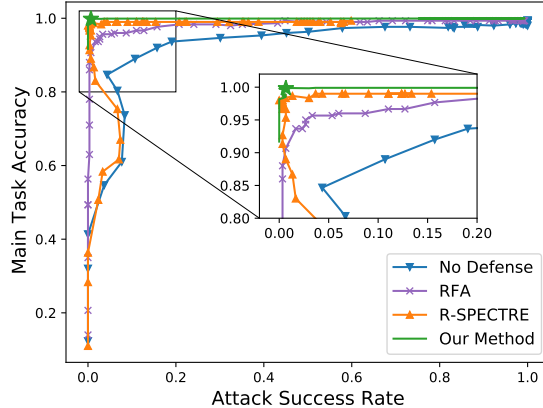


Figure 6: MTA-ASR tradeoff shows simple early stopping with no (other) defense far from the ideal (0,1) for  $\alpha = 0.15$ .

When  $\alpha = 0.15$ , the learning rate of backdoor samples is much smaller than the main task learning rate for all curves. However, the curves for early-stopping with no defense and early-stopped RFA still cannot achieve close-to-ideal tradeoffs.

## F.3 Synthetic heterogeneous clients

In synthetic heterogeneous EMNIST, each client receives shuffled images from 4 randomly selected classes with 25 samples per class. As shown in Table 4, it has a similar trend as the naturally heterogeneous dataset from the original EMNIST shown in Table 3.

Table 4: ASR under synthetic heterogeneous EMNIST

$\alpha$	Our Method with Sample-level Defense	Our Method	Our Method with User-level Defense
0.15	0.0134	0.0334	0.6756
0.25	0.0268	0.0401	0.7424
0.35	0.0535	0.0970	0.8127
0.45	0.0669	0.1305	0.9833

Further, we analyze the situation where the user-level version of our algorithm works. We construct variants of EMNIST dataset with different heterogeneity level  $h$ . We call the dataset  $h$ -heterogeneous if the first  $h$ -fraction of the overall training images are shuffled and evenly partitioned to each client, and for the remaining  $(1 - h)$ -fraction samples, each client receives shuffled images from 4 randomly selected classes with  $\lfloor 25(1 - h) \rfloor$  samples per class. For the adversarial clients, they also own 10 backdoor images. We fix the malicious rate as  $\alpha = 0.15\%$ . Table 5 shows the ASR of the user-level version of our algorithm under the dataset with different heterogeneity levels.

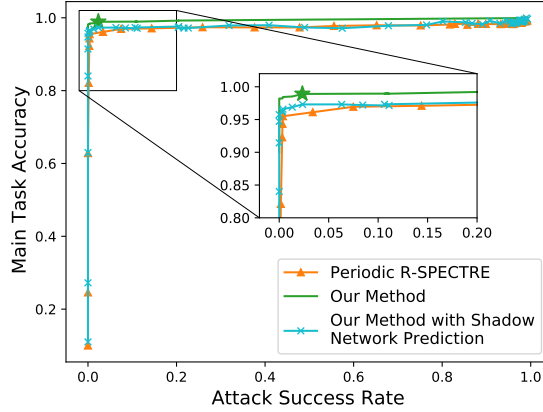
The ASR of the user-level version of our algorithm is smaller than 0.1 when  $h \leq 0.4$ , indicating that our user-level method can achieve the defense goal when under the dataset with low heterogeneity level. However, when the heterogeneity level is high, the malicious clients cannot be distinguished by the aggregated statistic over all local samples, which results in the failure of the user-level defense method.

## F.4 More experiments under the dynamic setting

Recall the initial phases  $e_1$  and  $e_2$  in Section 5.3. In the third phase  $e_3$ , for all clients, we reduce the number of samples with labels 0 and 1 to 10% of the original while keeping other samples at the same level in  $e_1$ , i.e., each client has

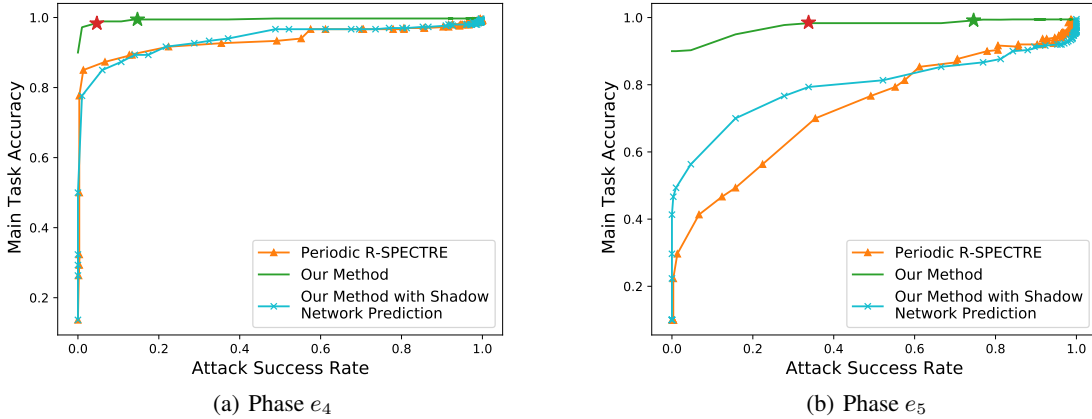
Table 5: ASR of Our Method in User-level Version with  $\alpha = 0.15$ 

Heterogeneity Level $h$	0	0.2	0.4	0.6	0.8	1
ASR	0.0216	0.0334	0.0969	0.2508	0.4816	0.6756

Figure 7: Analysis of MTA-ASR Tradeoff with  $\alpha = 0.15$  after distribution shift in phase  $e_3$ .

one image for label 0 and 1 respectively, and ten images for any other label. This tradeoff is shown in Figure 7. Since the number of samples with the target label  $\ell = 1$  is reduced, the learning rates of both the backdoor samples and the benign samples with the target label decrease. This is similar to the setting in Figure 6 except that the proportion of samples with the target label is smaller.

We also consider the case where the data distribution over malicious clients is fixed over time, which rarely happens in practice. In a new phase  $e_4$ , we let each benign client contain 5 images for label 0 and 1 respectively, and 10 images for any other label. In phase  $e_5$ , we further reduce the number of images each benign client contains for label 0 or 1 to one. However, the local dataset of each adversarial client is always fixed as the malicious dataset in  $e_1$ , i.e., 10 backdoor images in target label  $\ell = 1$  and 90 images for other labels. The MTA-ASR tradeoffs of phases  $e_4$  and  $e_5$  are shown in Fig.8

Figure 8: Analysis of MTA-ASR Tradeoff with  $\alpha = 0.15$  under Time-varying Dataset and Static Adversarial Clients

Our algorithm detects the data distribution change and renews the retraining period at the beginning of both phases. The MTA-ASR point our algorithm achieves is (0.9944, 0.1471) and (0.9937, 0.7458) in phases  $e_4$  and  $e_5$  respectively. The MTA-ASR tradeoffs of the comparing algorithms are much worse than ours in both phases.

Since the benign features with label 1 becomes more difficult to learn due to the leak of samples, and the proportion of backdoor samples among samples with target labels increases to 26% and 64% in phases  $e_4$  and  $e_5$  respectively, it is difficult to achieve the close-to-ideal MTA-ASR tradeoff. If we increase the convergence threshold  $\epsilon_2$  from 0.05% to 0.5% when determining the early-stopping point, we can obtain the new MTA-ASR point indicated by the red star as (0.9834, 0.0418) and (0.9834, 0.3378) in  $e_4$  and  $e_5$  respectively. By sacrificing a little bit MTA (around 0.01 in both cases), we can significantly reduce the ASR (around 0.1 in  $e_4$  and 0.4 in  $e_5$ ).

### F.5 Different backdoor trigger patterns

We focus on three different backdoor trigger patterns: diagonal trigger, random trigger, and periodic signal. The first two trigger patterns can be regarded as the pixel attack, while the last pattern belongs to the periodic attack [3]. The diagonal trigger consists of black pixels in the top left to bottom right diagonal, and as for the random trigger, 25 pixels are randomly selected from the image and fixed as the trigger pattern. For the periodic signal, we choose the sine signal with amplitude 8 and frequency of 10. As shown in Table 6, under the homogeneous EMNIST dataset, the ASR of our method is smaller than 0.06 in all cases, indicating our method can generalize to different types of backdoor attacks.

Table 6: ASR of Our Method under Different Trigger Patterns

$\alpha$	Diagonal Trigger	Random Trigger	Periodic Signal
0.15	0.0133	0.00 $\pm$ 0	0.00
0.25	0.0234	0.0067 $\pm$ 0.001	0.0201
0.35	0.0281	0.0268 $\pm$ 0.003	0.0367
0.45	0.0569	0.0533 $\pm$ 0.003	0.0585

### F.6 Defense against attacks with explicit evasion of anomaly detection [2]

For attack in [2], to explicitly evade the anomaly detection, adversarial clients modify their objective (loss) function by adding an anomaly detection term  $\mathcal{L}_{ano}$ :

$$\mathcal{L}_{model} = \gamma \mathcal{L}_{class} + (1 - \gamma) \mathcal{L}_{ano},$$

where  $\mathcal{L}_{class}$  represents the accuracy on both the main and backdoor tasks.  $\mathcal{L}_{ano}$  captures the type of anomaly detection they want to evade. In our setting,  $\mathcal{L}_{ano}$  accounts for the difference between the representations of backdoor samples and benign samples with target label  $\ell$ . The ASR of our algorithm under such attack is shown in Table 7 with different values of  $\gamma$ .

Table 7: ASR of Our Method under the Attack in [2]

$\alpha$	$\gamma = 0.4$	$\gamma = 0.6$	$\gamma = 0.8$	$\gamma = 1$
0.15	0.0100	0.0100	0.0067	0.0067
0.25	0.0133	0.0167	0.0133	0.0101
0.35	0.0201	0.0304	0.0368	0.0312
0.45	0.0367	0.0702	0.0635	0.0502

We can observe that with different  $\gamma$ , the ASR of our method is always smaller than or equal to 0.07 for the homogeneous EMNIST dataset, indicating that the attacks cannot succeed under our defense method even with explicit evasion of anomaly detection.

### F.7 Aggregation with noise

Our approach does not allow for secure aggregation, which may introduce privacy concerns. To this end, we consider the setting where all gradients and representations are corrupted with i.i.d. Gaussian noise  $\mathcal{N}(0, \sigma^2)$ , which is added to each coordinate before being uploaded from each client to the server. This is similar to Differentially-Private Stochastic

Gradient Descent (DP-SGD). We vary the variance  $\sigma^2$  from 0.001 to 1, and analyze the performance of our method in terms of (MTA, ASR) pairs under the homogeneous EMNIST dataset in Table 8.

Table 8: (MTA, ASR) Pair of Our Method under Different Noise Level

$\alpha$	$\sigma^2 = 0$	$\sigma^2 = 0.001$	$\sigma^2 = 0.01$	$\sigma^2 = 0.1$	$\sigma^2 = 1$
0.15	(0.997, 0.007)	(0.998, 0.003)	(0.994, 0.003)	(0.983, 0.000)	(0.873, 0.000)
0.25	(0.998, 0.010)	(0.996, 0.013)	(0.995, 0.007)	(0.983, 0.000)	(0.863, 0.000)
0.35	(0.998, 0.031)	(0.998, 0.031)	(0.994, 0.027)	(0.980, 0.000)	(0.852, 0.000)
0.45	(0.997, 0.050)	(0.996, 0.050)	(0.993, 0.042)	(0.980, 0.017)	(0.867, 0.000)

We can observe that as the noise level increases, both the MTA and ASR decrease. The intuition is that with large noise, the learning rate of the backdoor samples decreases, which makes the early-stopping framework more effective. However, the accuracy on main tasks also drops due to the noise. When  $\sigma^2 = 0.1$ , the ASR is 0 with  $\alpha \leq 0.35$ , while the MTA drops from around 0.997 to 0.98. With  $\sigma^2 = 0.01$ , the added noise can reduce the ASR while keeping MTA around 0.995.